Nuclear Engineering and Technology 50 (2018) 673–682

Contents lists available at ScienceDirect

Nuclear Engineering and Technology

journal homepage: www.elsevier.com/locate/net

Original Article

Uncertainty analysis of containment dose rate for core damage assessment in nuclear power plants

Guohua Wu [a, b, c], Jiejuan Tong [a, b, c], Yan Gao [d], Liguo Zhang [a, b, c, *], Yunfei Zhao [a, b, c]

[a] Institute of Nuclear and New Energy Technology, Tsinghua University, Beijing 100084, China
[b] Collaborative Innovation Center of Advanced Nuclear Energy Technology, Tsinghua University, Beijing 100084, China
[c] The Key Laboratory of Advanced Reactor Engineering and Safety of Ministry of Education, Beijing 100084, China
[d] China Ship Development and Design Center, Wuhan 430064, China

ARTICLE INFO

Article history:
Received 15 October 2017
Received in revised form
5 February 2018
Accepted 19 February 2018
Available online 14 March 2018

Keywords:
Containment Radiation Monitor
Core Damage Assessment
Nuclear Power Plants
Uncertainty Analysis

ABSTRACT

One of the most widely used methods to estimate core damage during a nuclear power plant accident is containment radiation measurement. The evolution of severe accidents is extremely complex, leading to uncertainty in the containment dose rate (CDR). Therefore, it is difficult to accurately determine core damage. This study proposes to conduct uncertainty analysis of CDR for core damage assessment. First, based on source term estimation, the Monte Carlo (MC) and point-kernel integration methods were used to estimate the probability density function of the CDR under different extents of core damage in accident scenarios with late containment failure. Second, the results were verified by comparing the results of both methods. The point-kernel integration method results were more dispersed than the MC results, and the MC method was used for both quantitative and qualitative analyses. Quantitative analysis indicated a linear relationship, rather than the expected proportional relationship, between the CDR and core damage fraction. The CDR distribution obeyed a logarithmic normal distribution in accidents with a small break in containment, but not in accidents with a large break in containment. A possible application of our analysis is a real-time core damage estimation program based on the CDR.
© 2018 Korean Nuclear Society, Published by Elsevier Korea LLC. This is an open access article under the CC BY-NC-ND license (http://creativecommons.org/licenses/by-nc-nd/4.0/).

1. Introduction

Currently, one of the most widely used methods for estimating the core damage state during a nuclear power plant (NPP) accident is containment radiation measurement. The core damage state is an important indicator of a nuclear emergency and also the key input for accident consequence assessment [1]. Because the core undergoes a very complicated physical and chemical progression during a severe accident, it is usually hard to directly obtain reliable information on the core damage state [2]. Therefore, manufacturers and regulatory agencies have proposed several methods for estimating the core damage, including core damage assessment guidance from Westinghouse [3], a response technical manual from the U.S. Nuclear Regulation Commission (NRC), and a generic assessment procedure from the International Atomic Energy Agency [4–6]. The core damage assessment guidance method for core damage estimation is shown in Fig. 1 [7]. The French Institute for Radiation Protection and Nuclear Safety proposed a triple diagnostics/triple prognostics (3D/3P) method in 1997 [8]; this method is widely used in nuclear emergency decision-making. The 3D/3P method focuses on the reactor core state and mainly relies on monitoring signals, such as containment dose rate (CDR). The 3D/3P method can also predict the reactor's subsequent core state [9].

In each method, the CDR is an almost indispensable indicator of the core damage state. The relationship between the CDR and core damage state is regarded as proportional and is now widely applied in NPPs [3–6]; however, no damage assessment studies have validated this relationship clearly.

The CDR in an accident is determined by the amount of radioactive material in the containment, namely the source term in the containment. The complexity of accidents, especially severe accidents [10], makes the source term highly uncertain; so, the CDR is likewise highly uncertain [11]. Therefore, this study investigated the uncertainty of the CDR because of a lack of such an analysis in the literature.

* *Corresponding author.* Institute of Nuclear and New Energy Technology, Tsinghua University, Beijing 100084, China.
E-mail addresses: wugh09@163.com (G. Wu), lgzhang@tsinghua.edu.cn (L. Zhang).

https://doi.org/10.1016/j.net.2018.02.004
1738-5733/© 2018 Korean Nuclear Society, Published by Elsevier Korea LLC. This is an open access article under the CC BY-NC-ND license (http://creativecommons.org/licenses/by-nc-nd/4.0/).

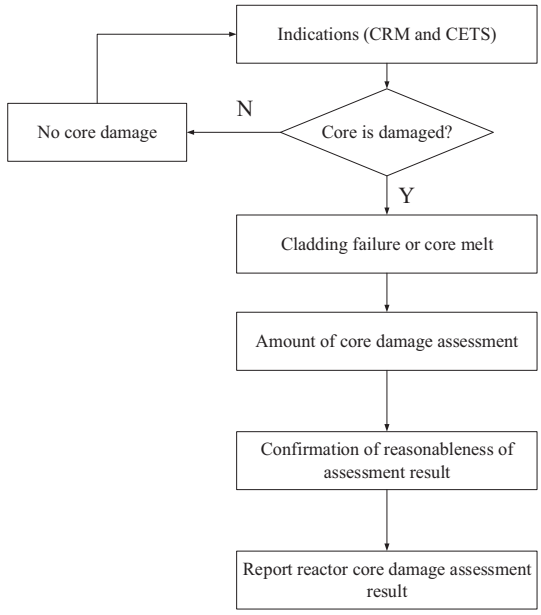

Fig. 1. Core damage assessment guidance method. CRM and CET are containment radiation measurement and core exit thermocouple, respectively.

Source term estimation has been studied to evaluate risk and to guide the design of NPPs. The United States Atomic Energy Commission started researching the source term and publishing reports such as WASH-740 [12], and its successor, the NRC, continued this research and published a series of reports about the source term, including WASH-1400, NUREG-1150, NUREG-1465, and NUREG-1228 [13–16]. France and Germany both launched similar research programs. After the Three Mile Island nuclear accident, the NRC established the Severe Accident Research Program (SARP) to analyze severe accidents and published reports such as NUREG/CR-5630 [19], which was the primary report describing the calculation of the source term for light water reactors. Meanwhile, many scholars have conducted studies for other types of NPPs [7,17]. Here, we used the outcomes of the SARP to conduct a CDR uncertainty estimation because NUREG/CR-5630 provides methods for evaluating the uncertainty of the source term.

This article first describes an uncertainty analysis of the CDR and presents an example that applies the CDR uncertainty to evaluate the core damage state for a specific reactor, the Surry NPP. This example may help advance the methodologies proposed by Westinghouse [3] and the International Atomic Energy Agency [4–6], in which the CDR is a critical indicator for assessing the core damage state and then estimating the source term. Other meaningful methods include, for instance, the rapid source term prediction applied to Sweden's Oskarshamn NPP [31], which was constructed using an NPP-specific Bayesian network model and probabilistic safety assessment model. The source term in the Swedish prediction method was previously estimated and identified by diagnosing the core state. The analysis presented here may supplement other methods. For Schéma d'Evaluation des Situations Accidentelles et Méthodes d'Evaluation (SESAME), which was developed by the French Institute for Nuclear Safety and Protection based on the 3D/3P method, the example provided here may be helpful for understanding the meaning of the standard CDR curves under different venting conditions. The Severe Accident Management Support Expert System was proposed to support severe accident management [32,33]. This method generally suggests a CDR threshold level. The example given here may aid in reducing variation and clarifying the uncertainty.

Section 2 discusses the parametric equation for source term estimation proposed by the SARP for the Surry NPP. To estimate the source term, equation parameters, such as the release fraction of radionuclides, decontamination by natural processes, and leakage, can be obtained by sampling their predefined probabilistic distribution function (PDF). Section 3 presents three accident scenarios, called accident progression bands (APBs), without early containment failure; CDR distributions for these accidents are constructed [6,18]. Section 4 summarizes and discusses the PDF of the CDRs. Section 5 presents a framework for real-time core damage estimation based on this study. Section 6 provides conclusions.

2. Methodology for source term estimation

The SARP uses a parametric equation to estimate the accident source term; therefore, each set of parameters will produce a different possible release of radioactive materials. The uncertainty of the source term is derived from the interactions among the uncertainties of the parameters in the equation.

Parametric uncertainty in the source term estimation model mainly comes from two aspects. One is the complexity of phenomena in an NPP core during an accident, and the other is the limited knowledge and experience that constrains our understanding of NPPs. Considerable subjective bias is inevitable; so, experts from different areas were convened to evaluate and produce distributions for the parameters that influence the source term estimation. The results are documented in NUREG-1150, which also applied the model to several NPPs, including the Surry NPP. The parametric PDF includes the subjective opinions of the experts [14], and it forms the basis of the uncertainty analysis of the accident source term. Parameters are sampled according to their PDF and used to calculate the source term. If source term samples are sufficiently abundant, a PDF can be built to examine the uncertainty of the source term. The CDR is determined by the source term within the containment; similarly, a PDF of the CDR can be built to reflect the uncertainty of the CDR.

To simplify the source term estimation, not all possible radionuclide releases are analyzed and calculated. Radionuclides are divided into nine radionuclide groups, namely inert gases, iodine, cesium, tellurium, strontium, ruthenium, lanthanum, cerium, and barium. The groupings are based on the principle that radionuclides in each group have similar physical and chemical properties and thus have similar release pathways.

2.1. Parametric equation of source term

Radioactive material within the containment of the Surry NPP is mainly removed by the spray system. In addition, core melt and concrete material falling into the bottom of containment are removed by rinsing the pit cover. The accumulation and deposition of suspended particles also play an important role in the release. The parametric equation can account for the following factors: releases from the pressure vessel and the volatility of iodine, interaction of the molten core with concrete, formation of high-pressure jets during release, direct atmospheric heating within the containment, and steam generator tube rupture. The parametric equations are then used to calculate radionuclide release [19]. Early and the late containment releases can be decomposed as follows:

$$STE_i = FCOR_i^* \left[(1 - FISG_i)^* FVES_i / DFE_i + (1 - FCOR_i)^* FPME \right] \quad (1)$$

$$STL_i = FPARTL^* (1 - FREM - FPME)^* FCCI_i^* (1 - FCOR_i) / DFL_i \quad (2)$$

The parameters are defined in Table 1. Each parameter has an assigned uncertainty, and the parameter distributions are

Table 1
Definitions of parameters in Eqs. (1) and (2).

Parameters	Meaning
STE	Early containment releases
STL	Late containment releases
$FCOR_i$	Fraction of iodine in the core released to the vessel before vessel break
$FISG_i$	Fraction of material released from the core vessel that enters the steam generators
$FVES_i$	Fraction of iodine released to the vessel that is subsequently released to the containment
DFE_i	Decontamination factor for reactor cooling system releases (such as sprays)
FPME	Fraction of radioactive material released by high-pressure jets
FPARTL	Fraction of core that participates in core concrete interaction (CCI)
FREM	Fraction of radionuclides retained in the pressure vessel, corresponding to the total amount of radionuclides present during late core release
$FCCI_i$	Fraction of fission products present in the core material at the start of CCI that is released to the containment during CCI
DFL_i	Decontamination factor for late releases

determined by systematic estimation and expert judgment. For different types of accidents, the parameter distribution may vary; so, it is very important to conduct uncertainty analysis.

2.2. Sampling volume of source term estimation

Before the CDR based on core release fractions can be calculated, the sampling volume, that is, the number of data points sampled, in the source term estimation program must first be determined. Sufficient sampling volume enhances the validity of the calculated distribution. In other words, the larger the sampling volume is, the closer the result is to the real distribution. But a larger sampling volume means more calculations and lower computational efficiency. Therefore, it is important to select an appropriate sampling volume.

In the source term estimation, Latin hypercube sampling is used to sample the parameter values [20]. Thereafter, the release fraction of different radionuclide groups is estimated according to Eqs. (1) and (2). By grouping these fractions into ascending value bins and then counting the items in each bin, we can create a frequency distribution of the release fractions. If the number of fraction values is sufficient, this frequency distribution becomes the PDF. In addition, different sampling volumes create different source term PDFs. The sampling volume was chosen by comparing these PDFs and their corresponding statistical properties. To estimate the sampling volume, we chose an accident progression with the following characteristics:

(1) Late containment failure,
(2) Spray system does not work,
(3) Core concrete interaction (CCI) occurs when the core is covered by water, and
(4) The containment has a small break.

The sampling volume was set at 1,000, 4,000, 8,000, and 16,000, and the release fraction PDFs of two radionuclide groups (the inert gases and iodine group) were calculated. The input of the parameter distributions in Eqs. (1) and (2) is described in NUREG/CR-5360 [19]. The PDFs of the inert gases group are shown in Fig. 2.

The results show that the PDFs at sampling volumes of 16,000 and 8,000 are very similar and their eigenvalues are almost the same. Therefore, it can be concluded that the PDFs at 16,000 can indicate a true distribution. At the same time, according to Table 2, when the sampling volume is 1,000, the distribution of the release fractions is close to that obtained with the sampling volume of 16,000, and the relative error of the eigenvalues is within 5%. Therefore, a larger sampling volume does not significantly improve the results, and, we concluded that the PDFs at a sampling volume of 1,000 could adequately reveal the distribution of radionuclide release characteristics. In view of the above analysis, a sampling volume of 1,000 was chosen for calculation of the release fractions of radionuclides in this study. The results for the PDFs of iodine release fractions let us draw a similar conclusion, as shown in Table 2.

3. Uncertainty analysis of CDR

3.1. Accident progression

Although early containment failure is also important for severe accident analysis, in this scenario, radionuclides are released into the environment very quickly, which leads to the loss of CDR monitoring signals. Because this study seeks to use those signals, we selected accident progression scenarios with late containment failure. Table 3 gives the accident characteristics and state of engineered safety features for the three late containment failure APBs used here.

In the source term estimation program, the core damage state is set to a specific value rather than being sampled from its PDF. To investigate the correspondence between the core damage state and the CDR, the CDR is estimated separately for core damage fractions of 1%, 10%, 90%, and 100%.

3.2. Assumption for calculating the CDR

The core inventory used here was provided by the radiological assessment system for consequence analysis (RASCAL) consequence analysis code according to a typical American NPP rated at about 3,000 MWt [21]. As the amount of specific radionuclides can decrease or increase due to decay during the release, the effects of decay must be taken into account in calculating the CDR. RASCAL incorporates a decay process estimation method.

Given the characteristics of the radioactive material and structure of the containment, the gamma dose rate at a given detector position can be calculated. In this study, we used two methods to calculate the CDR, the Monte Carlo (MC) method and the point-kernel integration (PKI) method [22,23].

The simplified geometrical structure of the Surry NPP is shown in Fig. 3 [24]. Because the containment structure, the phenomena during a severe accident, and the parameter distribution for describing the mechanism of a pressurized water reactor are similar for all reactors of this type, it is feasible to make general conclusions by studying a specific case. But these results cannot necessarily be applied to different types of reactors, especially heavy water reactors or early boiling water reactors; so, for any other specific quantitative application, the geometry, phenomena, and parameters must be carefully checked and adjusted. In Fig. 3, the shaded area represents the volume occupied by the structure and equipment; the blank area is the free volume of the containment; and “A” indicates the position of the detector (the number and location of measuring points are different for other types of NPPs). To simplify the calculation of the CDR, the following basic assumptions were made [14]:

(1) The containment is not bypassed.
(2) Only the CDR attributable to radioactive material released into the containment is considered, regardless of other dose sources that may be present.

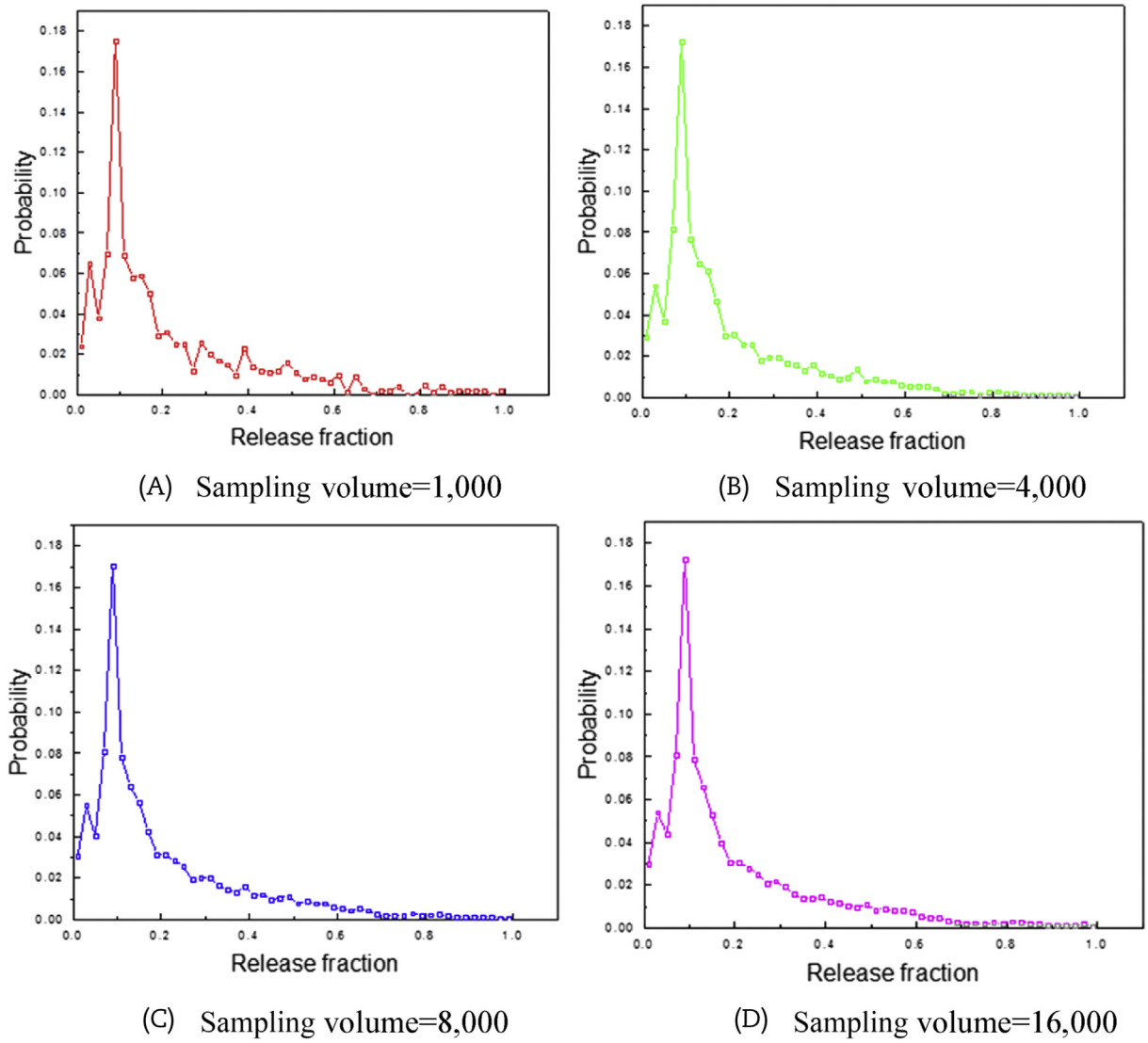

Fig. 2. PDF of release fractions of the inert gases group.
(A) Sampling volume = 1,000. (B) Sampling volume = 4,000. (C) Sampling volume = 8,000. (D) Sampling volume = 16,000.

Table 2
Characteristic values of radionuclides in the inert gases group and iodine group.

Analysis parameters	Inert gases group				Iodine group			
Sampling volume	1000	4000	8000	16000	1000	4000	8000	16000
Mean value	0.21	0.21	0.212	0.21	0.61	0.6	0.6	0.6
Standard deviation	0.19	0.18	0.18	0.19	0.32	0.32	0.32	0.32
Median	0.14	0.13	0.13	0.13	0.7	0.69	0.68	0.68
10%	0.05	0.05	0.05	0.05	0.11	0.11	0.11	0.11
90%	0.49	0.48	0.48	0.49	0.98	0.98	0.98	0.98

Table 3
Descriptions of accident scenarios.

APB	Description
APB1	Late containment failure, spray system does not run, CCI occurs without water present, and accident with a large break in containment
APB2	Late containment failure, spray system does not run, CCI occurs with core covered in water, and accident with a small break in containment
APB3	Late containment failure, spray system does not run, CCI occurs with core covered in water, and accident with a small break in containment

APB, accident progression band; CCI, core concrete interaction.

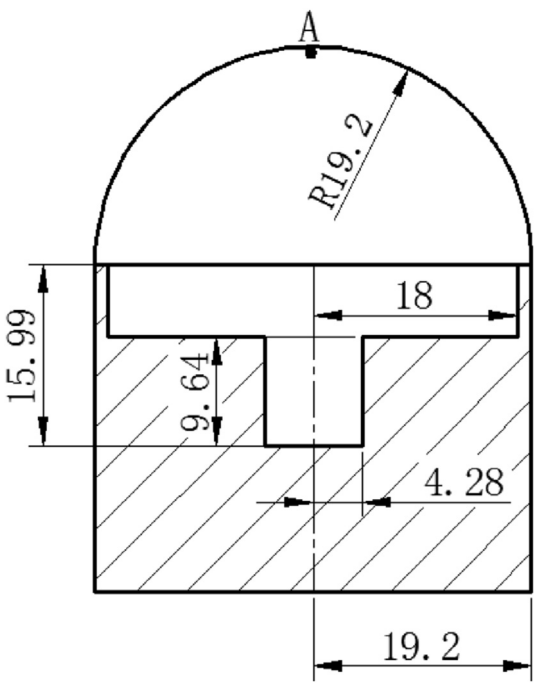

Fig. 3. Simplified schematic of the containment model (Unit: m).

(3) Radioactive material released from the core into the containment is distributed evenly in the free space of the containment.
(4) Radioactive material removed by the spray system is not included in the dose rate calculation.
(5) The detector has a straight line of sight to any location within the containment free space.
(6) Radioactive material can be removed by multiple processes, including wall deposition, heat transfer, and diffusion electrophoresis. Deposition of radioactive material is evenly distributed over all inner surfaces within the containment, and the deposited material contributes to the CDR.
(7) Other equipment systems are simplified by treating them as concrete within the containment, which means that the only materials involved in the modeling are air and concrete.

3.3. Calculation method for CDR

For comparison and verification, both the MC and PKI methods were used to calculate the CDR [25,26]. Before the dose rate estimation, X/γ spectra, including energy and corresponding intensity from radioactivity in the containment, were built according to the decay scheme and activity of radionuclides and the structure of the Surry containment (Fig. 3). The MC method is widely used in stochastic processes such as neutron transport [27] and atmospheric dispersion modeling [28]. In this study, the Monte Carlo N-Particle Transport Code (MCNP) was used to track photon transport and calculate the normalized dose rate. Then, the normalized dose rate was multiplied by the intensity of photons to obtain the CDR.

The PKI method is a macroscopic method for calculating gamma and neutron doses. Its basic approach is to disperse a radiation source into a number of points. The dose rate from each point is calculated, and then the total dose rate can be integrated by Eq. (3) [29].

$$D = \int_E \int_V \frac{S(r,E)\cdot B(\mu|r-r'|)\cdot\eta}{4\pi|r-r'|^2} e^{-\mu|r-r'|} dVdE \tag{3}$$

In the PKI method, the free volume and containment surfaces where radioactive material exists were differentiated into elements small enough to be treated as point sources. The CDR of each scenario is the summation of contributions from all these point sources.

Each estimated source term result was put into the MCNP and PKI models of Surry to calculate the CDR; two CDR values were obtained for each core damage fraction and for each of the three APBs. The accuracy was checked by comparing the results from the two methods. The fraction of radioactive material release, namely the source term, was the uncertainty. As a result, the CDR is uncertain. Fig. 4 provides a flow chart of this process.

4. Analysis and discussion of results

4.1. Calculation results based on MCNP and PKI methods

The CDR was calculated using the MCNP and PKI methods for three scenarios and four core damage states. The CDR distributions are shown in Figs. 5–7 for APB1, APB2, and APB3, respectively; in each figure, the MCNP and PKI results are given on the left and right sides, respectively. The X-axis is the dose rate, and the Y-axis is the corresponding frequency fraction. The 1%, 10%, 90%, and 100% curves represent the core damage fraction. The default curve represents the case in which the core damage fraction is also a random variable with a specific distribution.

4.2. Analysis of results

4.2.1. Comparison of results of the two methods

The PDFs of the CDR estimations obtained using the MCNP and PKI methods were approximately the same, so were the eigenvalues of the two methods. The mean values of the two methods for each APB and damage fraction are shown in Table 4; as mentioned before, the "default" column represents the case in which the core damage fraction is also a sampling distribution. The other columns correspond to the indicated core damage fraction. The mean values

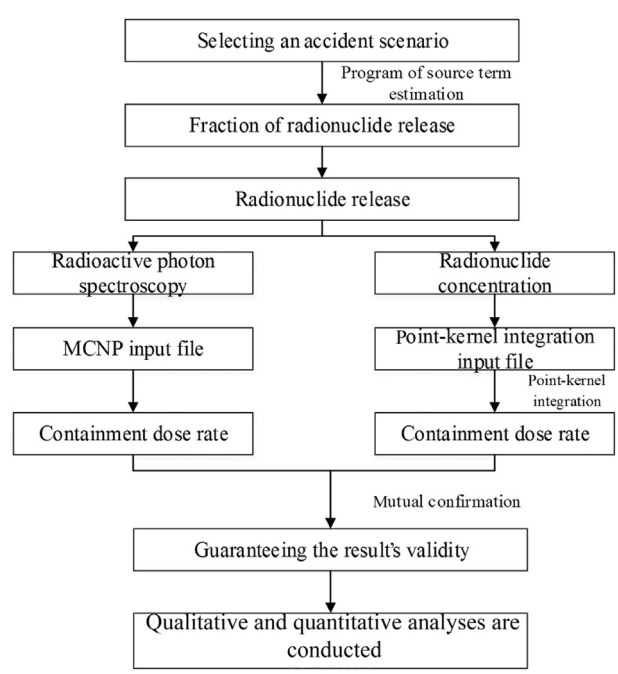

Fig. 4. Flow chart of uncertainty analysis of the CDR.
CDR, containment dose rate; MCNP, Monte Carlo N-Particle Transport Code.

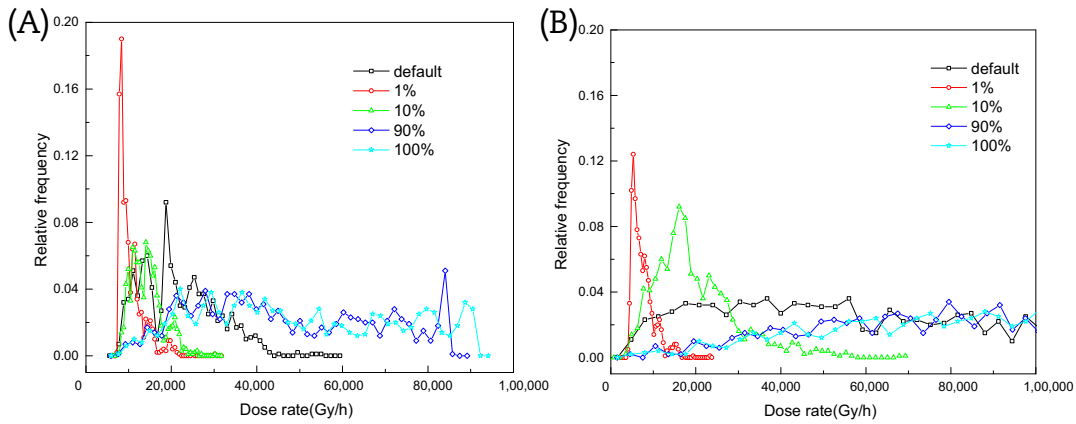

Fig. 5. Probability density function of CDR for APB1 based on MCNP and PKI methods. (A) MCNP method. (B) PKI method.
APB, accident progression band; CDR, containment dose rate; MCNP, Monte Carlo N-Particle Transport Code; PKI, point-kernel integration.

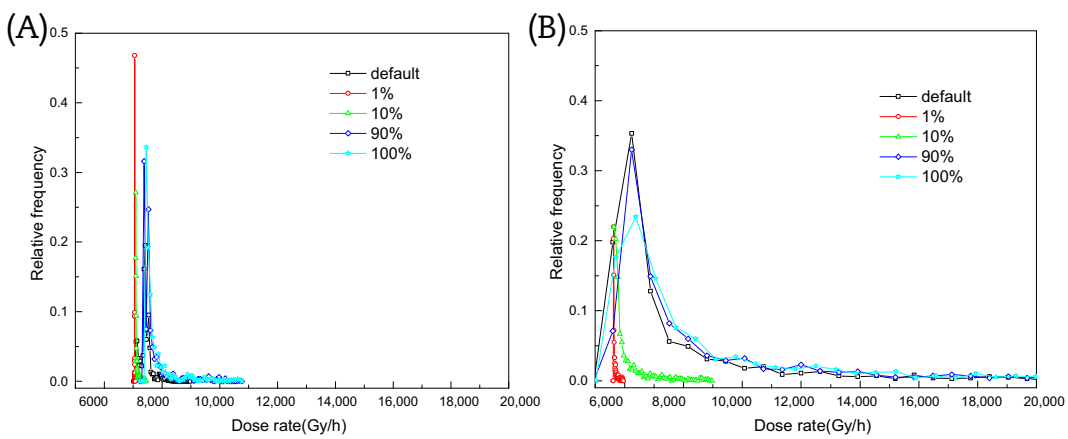

Fig. 6. Probability density function of CDR for APB2 based on MCNP and PKI methods. (A) MCNP method. (B) PKI method.
APB, accident progression band; CDR, containment dose rate; MCNP, Monte Carlo N-Particle Transport Code; PKI, point-kernel integration.

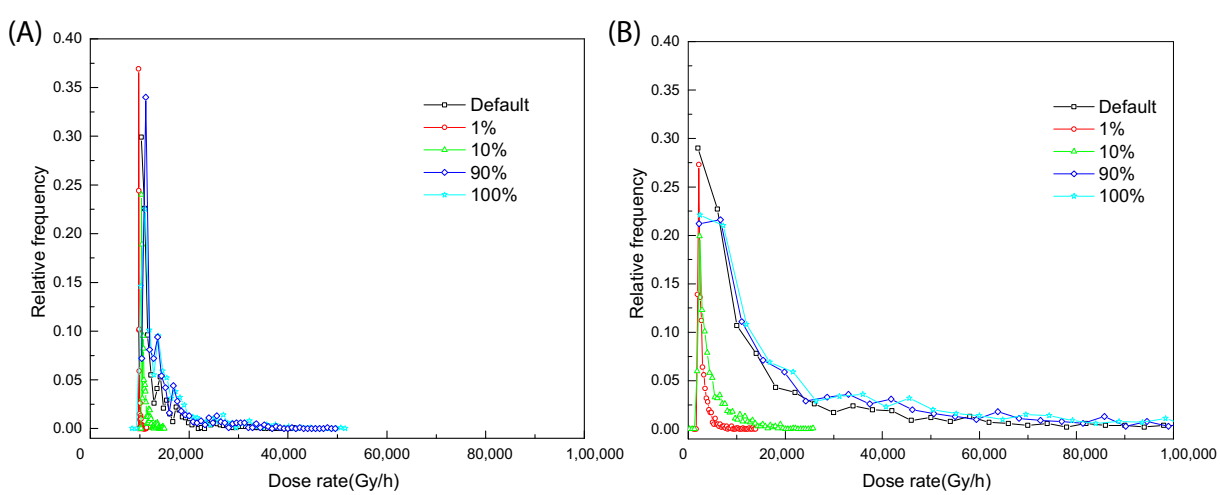

Fig. 7. Probability density function of CDR for APB3 based on MCNP and PKI methods. (A) MCNP method. (B) PKI method.
APB, accident progression band; CDR, containment dose rate; MCNP, Monte Carlo N-Particle Transport Code; PKI, point-kernel integration.

Table 4
Comparison of mean values of probability density function for different APBs (Unit: Gy/h).

Accident progression band	Methods	Core damage fraction				
		Default	1%	10%	90%	100%
APB1	MC	2.17E+04	1.04E+04	1.42E+04	4.62E+04	0.50E+05
	PKI	6.48E+04	0.76E+04	2.00E+04	9.29E+04	1.02E+05
APB2	MC	7.43E+03	7.05E+03	7.12E+03	7.69E+03	7.76E+03
	PKI	8.01E+03	5.66E+03	6.01E+03	9.15E+03	8.01E+03
APB3	MC	1.30E+04	9.88E+03	1.09E+04	1.45E+04	1.49E+04
	PKI	1.81E+04	2.92E+03	5.12E+03	2.46E+04	2.71E+04

APB, accident progression band; MC, Monte Carlo; PKI, point-kernel integration.

of different APBs listed in Table 4 show no systematic deviation between values determined by the MCNP and PKI methods, indicating that both methods are effective for evaluating the uncertainty of the CDRs. In addition, discussion of mean values may help us understand how to build a simplified model to assess core damage. Therefore, we concluded that the results obtained using the two methods are basically consistent with respect to trend and distribution.

4.2.2. Qualitative analysis

The distribution of the CDR has different degrees of fluctuation because it is impossible to obtain an actual distribution of the CDR. The qualitative analysis, which mainly focused on the trends and important eigenvalues of the distribution, produced two main points.

(1) The CDR showed a certain distribution for the different core damage fractions based on each accident progression scenario. Comparison of the same core damage fraction across the accident scenarios shows that the CDR distribution at 1% core damage is very concentrated. The CDR at 100% core damage is the most dispersed, meaning that the CDR has maximum uncertainty. In severe accidents, a greater extent of core damage increases the uncertainty of the parameters.
(2) In APB1, an accident with a large break in containment, it was found that in addition to the distribution concentration at a core damage fraction of 1%, the CDR had greater uncertainty. In APB2, an accident with a small break in containment, a different core damage fraction had the most obvious maximum relative frequency, and the distribution is mainly concentrated around the most probable dose rate value. For the other accident with a small break in containment, APB3, it was found that the CDR distribution is similar to that of APB2. Therefore, the main source of uncertainty in APB1 is a large break in containment. This means that, with other conditions being the same, a larger break in the containment causes greater uncertainty in the CDR.

4.2.3. Quantitative analysis

(1) Relationship between core damage fraction and CDR

To reduce the uncertainty of the CDR, the mean of 1,000 CDR values was used to establish the relationship between the core damage fraction and CDR. It is difficult to analyze the relationship between the CDR and the core damage fraction based on the distribution. Therefore, the mean value of the CDR was calculated, as shown in Table 4, and then different accidents were selected to calculate the relationship between the core damage fraction and CDR. With an assumed proportional relationship, linear fitting was carried out. The linear fitting curve of APB1 is shown in Fig. 8.

The linear fitting parameters for APB1, APB2, and APB3, based on the MCNP method, are shown in Table 5. The R^2 values range from 0% to 100%, where a higher R^2 value indicates a more useful fitting [29,30], and a lower R^2, 70% or less, indicates a fitting that is not representative of the function.

In this study, APB1, APB2, and APB3 fitting analyses showed that the relationship between the CDR and core damage fraction is linear rather than proportional, as was expected. Possible reasons are

(A) The linear relationship between the mean value of the CDR and the core damage fraction does not indicate that the calculated intercept will exist in actual accidents. Rather, it demonstrates that when core damage occurs, the CDR is relatively large.
(B) The CDR has a certain degree of uncertainty corresponding to the core damage state. Therefore, the rate density distribution has a considerable width, and the CDR intercept is still very low when core damage occurs.
(2) Calculation of CDR distribution

As shown in Figs. 5 and 6, the MCNP results are more concentrated than the PKI results. This indicates that the MCNP method for quantitative analysis produces a tighter distribution than does the

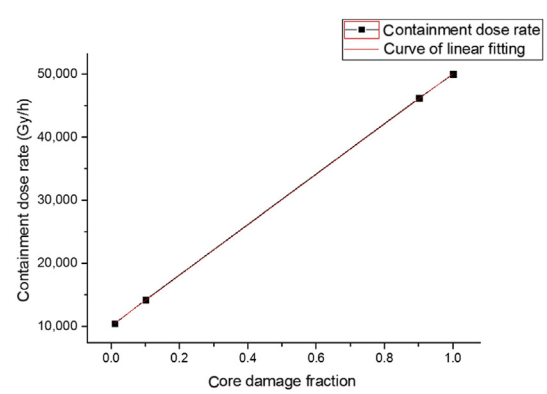

Fig. 8. The curve linear fitting of APB1.
APB, accident progression band.

Table 5
Linear fitting parameters for APB1, APB2, and APB3 (Unit: Gy/h).

	Methods	APB1	APB2	APB3
MC	Slope	39955	711.3	4888.8
	Intercept	10136	7047.1	10097
	R^2	0.999	0.999	0.988
PKI	Slope	93670	2981	24395
	Intercept	8555	5709	2676
	R^2	0.999	0.810	0.999

APB, accident progression band; MC, Monte Carlo; PKI, point-kernel integration.

PKI method; therefore, MCNP results were used for the quantitative analysis. The purpose of this study is to find a function that can represent the uncertainty distribution of the CDR and lay a foundation for a subsequent engineering application. The qualitative analysis showed that the greater the degree of damage, the greater the uncertainty and error in the calculated distribution. Therefore, the scenario with a small break in containment, ABP2, was chosen as the uncertainty distribution for exploring the function of the CDR distribution.

According to mathematical analysis and fitting results, a logarithmic normal distribution was used to achieve a function representing the distribution of the CDR. The logarithmic normal distribution function can be given as Eq. (4).

$$y = y0 + \frac{A}{\sqrt{2\pi}wx}\exp^{\left(-\frac{\ln(x/xc)^2}{2w^2}\right)} \tag{4}$$

To show the fitting effect, the better fitting curves of APB2 are shown in Figs. 9 and 10.

Fitting was carried out according to the PDFs of the CDR corresponding to ABP1, ABP2, and ABP3. The logarithmic normal fitting parameters are shown in Table 6.

In Table 6, APB2 and ABP3 have better fitting effects as the logarithmic normal distribution is valid only with a small break in containment. According to the results of quantitative analysis, we can see the correctness of the qualitative analysis results: scenario ABP1 has a large break in containment, and its CDR distribution has greater uncertainty. ABP2 and APB3 are accidents with a small break in containment, and the effect of logarithmic normal distribution fitting is better. Based on this analysis, we conclude that the uncertainty analysis of the CDR in accidents with a small break in containment is subject to a logarithmic normal distribution.

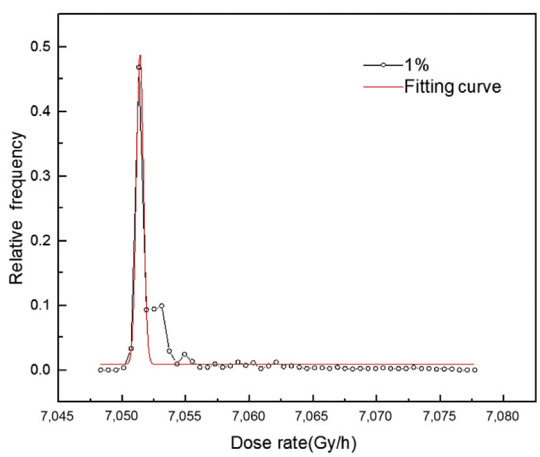

Fig. 9. Fitting curve of the CDR for APB2 with 1% core damage.
APB, accident progression band; CDR, containment dose rate.

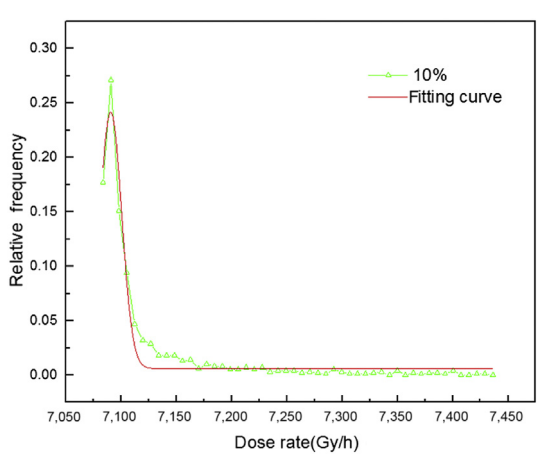

Fig. 10. Fitting curve of the CDR for APB2 with 10% core damage.
APB, accident progression band; CDR, containment dose rate.

4.2.4. Summary

The qualitative and quantitative analyses reached the same conclusion that the CDR distribution has a greater uncertainty in accidents with a large break in containment. The qualitative and quantitative analyses can be summarized as follows:

(1) The CDR distribution has greater uncertainty for accidents involving a large break in containment and increased core damage fractions;
(2) The CDR and core damage fraction relationship has a linear correlation, not the expected proportional one;
(3) Uncertainty analysis of the CDR in accidents with a small break in containment is subject to logarithmic normal distribution.

5. Method for real-time dynamic core damage estimation

This study used the CDR uncertainty analysis described previously to develop a method for evaluating the core damage state in real time. Because the core damage estimation does not take time passage into account, as shown in Fig. 1, and the method of core damage estimation has uncertainty, we propose dynamic core damage estimation. The proposed method uses a 1,000-s time series to conduct core damage estimation. This approach can eliminate some of the uncertainty shown in Fig. 6 and can be used to calculate the distribution of the CDR. The method uses the 1,000-s series to achieve the CDR distribution needed to evaluate an accident and uses the mean value to estimate core damage. The procedure is illustrated in Fig. 11 and described step by step below:

Step 1 Real-time monitoring data are transmitted and stored at the NPP. By obtaining the monitoring signal from the digital control system, the CDR parameter is updated in real time.
Step 2 A CDR threshold is established and compared with the CDR updates in real time. Once the CDR exceeds the threshold, the value is stored in a dynamic array with a length of 1,000 (to match the sampling volume introduced in Section 2.2 and optimize the accuracy and speed of the calculation).
Step 3 When the data length reaches 1,000 values, the average of these 1,000 values is calculated. According to the results of the simulation experiment in Section 4.2, the average value can be used to estimate the core damage fraction. The 1,000 data points are fitted to a logarithmic normal distribution to obtain the parameters of the results. MCNP and PKI results are compared for confirmation.
Step 4 As time goes on, especially late in severe accidents, the core damage fraction will continue to increase; so, the evaluation results are also updated in real time. When the 1,001st data point enters the dynamic array, the last data point is removed. The dynamic array ensures real-time data updates and the accuracy of the core damage fraction value. Steps 1–3 are repeated using the latest 1,000 data points.
Step 5 Emergency responders make decisions according to real-time analysis results, including core damage fraction.

The advantages of this method are as follows: (1) The calculation of the core damage fraction can be updated in real time, and

Table 6
Values of logarithmic normal fitting parameters.

Analysis parameters	APB1				APB2				APB3			
	1%	10%	90%	100%	1%	10%	90%	100%	1%	10%	90%	100%
xc	8.46E+03	1.37E+04	5.69E+04	3.95E+06	7.05E+03	7.09E+03	7.46E+03	7.48E+03	9.80E+03	1.04E+04	1.10E+04	1.12E+04
w	8.64E-02	2.72E-01	7.56E-01	4.28E-02	3.97E-05	1.39E-03	1.48E-02	5.07E-03	1.94E-03	2.87E-03	7.29E-02	4.02E-02
A	296.00	547.74	2587.13	8196.76	0.34	5.84	56.36	38.27	21.43	61.23	429.41	371.33
y0	8.62E-03	−1.02E-03	-2.1E-03	2.00E-02	8.62E-03	6.02E-03	4.46E-03	9.42E-03	7.43E-03	1.19E-02	1.02E-02	1.07E-02
R^2	0.746	0.87	0.412	−0.065	0.918	0.959	0.615	0.857	0.883	0.787	0.792	0.857

APB, accident progression band.

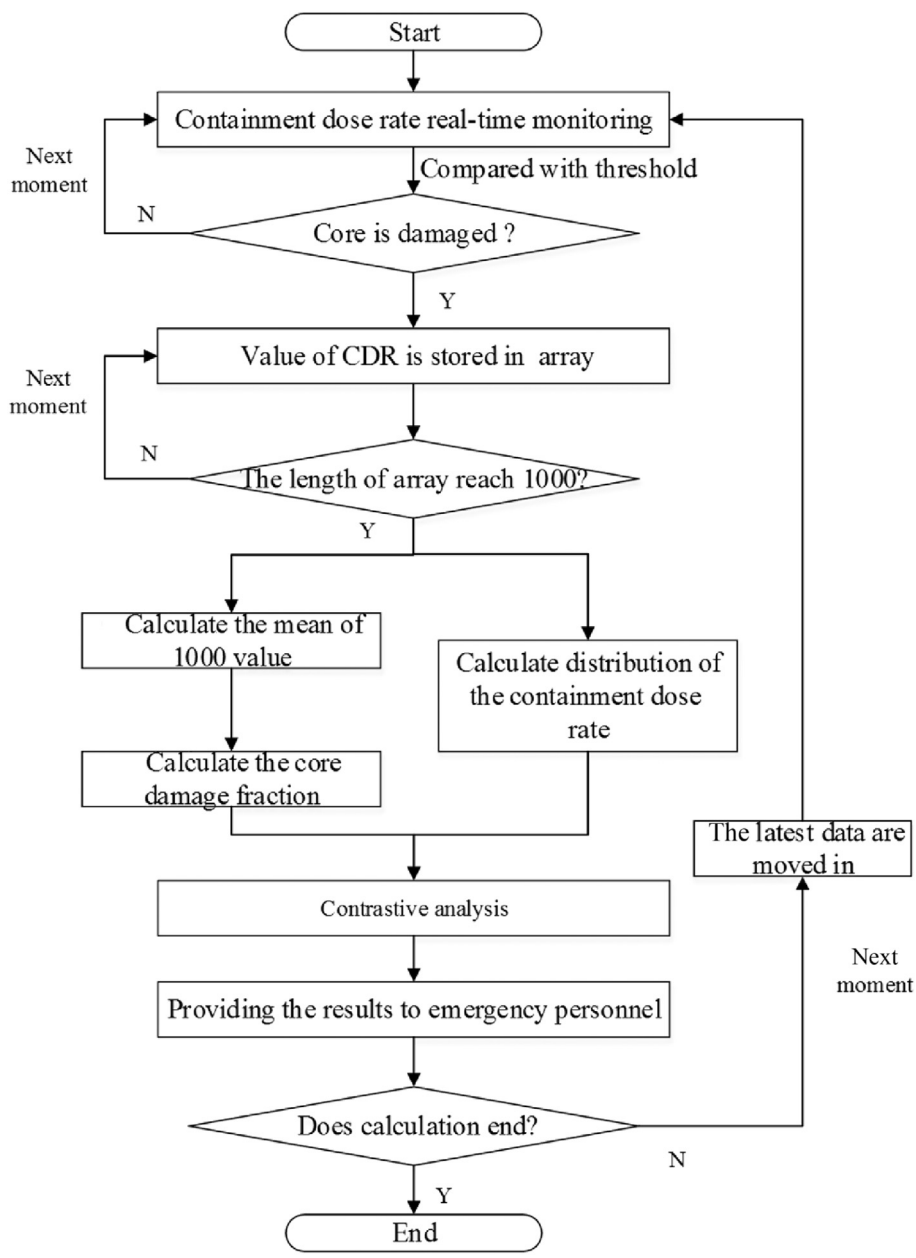

Fig. 11. Flow chart of real-time core damage estimation.
CDR, containment dose rate.

the calculation process is simplified by basing it on a threshold. (2) The history and latest data are used for calculations to assess the core damage fraction.

6. Conclusion

Based on the uncertainty analysis method of NUREG-1150, we used the Surry NPP as a case study to check the distribution of the CDR under different core damage fractions for three accident scenarios. After the source term estimation, the MC and PKI methods were used to evaluate the CDR, and then, PDFs of the CDR for different APBs were accumulated.

One can clearly determine the possible characteristics of the CDR and the relationship between CDR and core damage state when a severe accident occurs. This provides the operator or emergency worker with an adequate assessment, allowing them to avoid hasty conclusions. In addition, the uncertainty evaluation revealed that the proportional relation predicted in some studies is correct only when the mean value or the expected CDR distribution is taken into account. Even so, further investigation will reveal new ways to create an approximate relation between the CDR and core damage for possible application in uncertainty analysis. Section 5 describes only one example of model application.

This study mainly considered the uncertainty of radioactive material released into the containment, and it did not take into account other factors that may increase the CDR uncertainty. In addition, we analyzed only three types of accident progression, and more simulations are required. Finally, a method for real-time evaluation of the core damage was proposed. It is expected that a software program for evaluating the core damage fraction with the CDR can be developed and applied to nuclear emergency decision-making.

Conflict of interest

There is no conflict of interest.

Acknowledgments

This work is supported by the National Science and Technology Major Project (Grant No. ZX06901) and Nuclear Energy Development Project.

References

[1] C.M. Allison, J.K. Hohorst, An assessment of effectiveness of core exit temperatures with respect to PWR core damage state using RELAP/SCDAPSIM/MOD3.4, Nucl. Eng. Des. 238 (2008) 1547–1560.
[2] U.S. Nuclear Regulatory Commission (NRC), Clarification of TMI Action Plan Requirements, NUREG-0737, Nuclear Regulatory Commission, U.S., 1980.
[3] U.S. Westinghouse Electric Company LLC, Westinghouse Owners Group Post Accident Core Damage Assessment Methodology, Westinghouse Electric Company LLC, U.S., 1984.
[4] U.S. Nuclear Regulatory Commission, Modifications Proposed by the Westinghouse Owners Group to the Core Damage Assessment Guidelines and Post Accident Sampling System Requirements, Nuclear Regulatory Commission, U.S., 1999.
[5] T. McKenna, J. Trefethen, K. Gant, et al., RTM-96 (NUREG/BR-0150). Response Technical Manual, vol. 1, Nuclear Regulatory Commission, U.S., 1996.
[6] International Atomic Energy Agency, Generic Assessment Procedures for Determining Protective Actions during a Reactor Accident, IAEA-TECDOC-955, International Atomic Energy Agency, Vienna, 1997.
[7] Y. Zhao, L. Zhang, J. Tong, et al., Development of rapid atmospheric source term estimation system for AP1000 nuclear power plant, Prog. Nucl. Energy 81 (2015) 264–275.
[8] D. Winter, J.M. Agator, Utilisation of the SESAME system for diagnosis and prognosis of plant status during an emergency in a French PWR, Radiat. Protect. Dosim. 73 (1997) 273–276.
[9] Feng Jun-yi, Tong Jie-juan, Qu Jingyuan, Research and application of SESAME system, Sci. Technol. Rev. 24 (2006) 61–64 (in Chinese).
[10] B.R. Sehgal, Nuclear Safety in Light Water Reactors: Severe Accident Phenomenology, 2012.
[11] Lutz R J. Westinghouse Owners Group Core Damage Assessment Guidance. Pittsburgh: Westinghouse Electric Company LLC. McGuire S A, Ramsdell J V, Athey G F, 2007. RASCAL 3.0.5: Description of Models and Methods, NUREG-1887. U.S. Nuclear Regulatory Commission, 1999.
[12] U.S. Atomic Energy Commission, Possibilities T. Consequences of Major Accidents in Large Nuclear Power Plants, WASH 740, Atomic Energy Commission, U.S., 1957.
[13] H.W. Lewis, R.J. Budnitz, W.D. Rowe, et al., Reactor Safety Study: an Assessment Accident Risks in U.S. Commercial Nuclear Power Plants, WASH-1400 (NUREG/CR-0400), Nuclear Regulatory Commission, U.S., 1975.
[14] T.J. McKenna, J.G. Giitter, Source Term Estimation during Incident Response to Severe Nuclear Power Plant Accidents, NUREG 1228, Nuclear Regulatory Commission, U.S., 1988.
[15] D. Ross, J. Murphy, M. Cunningham, et al., Severe Accident Risks: an Assessment for Five U.S. Nuclear Power Plants, NUREG-1150, Nuclear Regulatory Commission, U.S, 1990.
[16] L. Soffer, S.B. Burson, C.M. Ferrell, Accident Source Terms for Light-water Nuclear Power Plants, NUREG-1465, Nuclear Regulatory Commission, U.S., 1995.
[17] M. Vela-García, K. Simola, Evaluation of JRC source term methodology using MAAP5 as a fast-running crisis tool for a BWR4 Mark I reactor, Annals of Nuclear Energy 96 (2016) 446–454.
[18] J.F. Li, Z.Q. Shi, X.Y. Wang, PWR containment radiation levels calculation related to core conditions, Nucl. Sci. Eng 24 (2004) 31–35 (in Chinese).
[19] H.N. Jow, W.B. Murfin, J.D. Johnson, XSOR Codes User's Manual, NUREG/CR—5360, Nuclear Regulatory Commission, U.S., 1993.
[20] Michael D. Shields, Jiaxin Zhang, The generalization of Latin hypercube sampling, Reliability Engineering and System Safety 148 (2016) 96–108.
[21] S.A. McGuire, J.V. Ramsdell, G.F. Athey, RASCAL 3.0.5: Description of Models and Methods, NUREG-1887, NRC, U.S., 2007.
[22] F.B. Judith, MCNP—a General Monte Carlo N—particle Transport Code, University of California, U.S, 2000.
[23] U.S. Nuclear Regulatory Commission, The Mesorad Dose Assessment Model, NUREG/CR-4000, Nuclear Regulatory Commission, U.S., 1986.
[24] U.S. Nuclear Regulatory Commission, State-of-the-Art Reactor Consequence Analyses Project, Nuclear Regulatory Commission, 2013.
[25] J.H. Hubbell, S.M. Seltzer, Tables of X-Ray Mass Attenuation Coefficients and Mass Energy-absorption Coefficients from 1 KeV to 20 MeV for Elements Z = 1 to 92 and 48 Additional Substances of Dosimetric Interest, National Institute of Standards and Technology, U.S., 1996.
[26] International Atomic Energy Agency (IAEA), Generic Models and Parameters for Assessing the Environment Transfer of Radionuclides from Routine Releases, International Atomic Energy Agency, Vienna, 1982.
[27] R. Henry, I. Tiselj, L. Snoj, CFD/Monte-Carlo neutron transport coupling scheme, application to TRIGA reactor, Ann. Nucl. Energy 110 (2017) 36–47.
[28] G. Katsiolides, E.H. Müller, R. Scheichl, et al., Multilevel Monte Carlo and Improved Timestepping Methods in Atmospheric Dispersion Modelling, 2016.
[29] R.G. Carpenter, Principles and procedures of statistics with special reference to the biological sciences, Ann. N. Y. Acad. Sci. 682 (1960) 283–295.
[30] A.C. Cameron, F.A.G. Windmeijer, An R-squared measure of goodness of fit for some common nonlinear regression models, J. Econom. 77 (1997) 329–342.
[31] M. Knochenhauer, V. Hedtjärn Swaling, F. Di Dedda, F. Hansson, S. Sjökvist, K. Sunnegård, Using Bayesian Belief Network (BBN) Modelling for Rapid Source Term Prediction – Final Report, NKS-293, ISBN 978-87-7893-369-0, 2013.
[32] S.Y. Park, K.I. Ahn, SAMEX: a severe accident management support expert, Ann. Nucl. Energy 37 (2010) 1067–1075.
[33] K.I. Ahn, S.Y. Park, Development of a risk-informed diagnostics and prognostics system to support severe accident management, Nucl. Eng. Des 239 (2009) 2119–2133.